



Optimizing the shape of the M10 engine's injector head methane circuit using RBF mesh morphing

by Ubaldo Cella¹, Viviana Ferretti², Andrea Terracciano², Daniele Liuzzi², Daniele Drigo², Francesco Di Matteo³, Marco Evangelos Biancolini¹

1. RBF Morph - 2. AVIO - 3. ESA

This article is based on a collaboration between RBF Morph and AVIO to configure a numerical optimization procedure to improve the Vega E M10 engine's performance by optimizing the methane circuit of the injector head. Vega E (Evolution) is the new three-stage satellite launch vehicle (see above) for a project coordinated by ESA (European Space Agency) to qualify the Vega C's successor. The Vega E's maiden flight is scheduled for 2026.

The M10 (see Fig. 1), which will use liquid oxygen and liquid methane as propellants, is a new-generation more environmentally friendly engine for the final stage of the launcher, and was developed and built by Avio

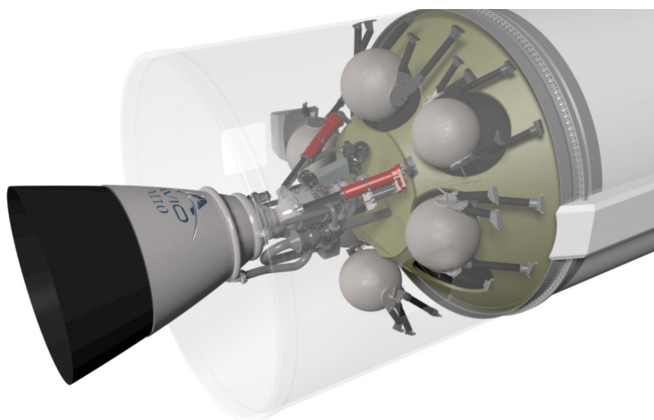


Fig. 1. The M10 engine.

in Colleferro in Italy. It is a 10-tonne LOX/LCH₄-class cryogenic liquid rocket engine and is the first European engine to use methane. The design team, led by Avio, involves a consortium of companies from Belgium, the Czech Republic, Switzerland, France, Austria, and Romania. The design objective for this activity was to reduce the pressure drop between the inlet of the manifold and the outlet of the engine combustion chamber with a constraint on the maximum temperature of the firing plate.

What is the problem to be solved?

The fluid domain configuration used to model the injector head is shown in Fig. 2. The inlet is on the methane collector at the side of the manifold. The flow enters the dome through two rows of holes and through another series of channels with different shapes.

Steady RANS analyses using the realizable turbulent $k-\epsilon$ model with standard wall functions were run. Mass flow rate and temperature were imposed at the inlet. A fixed pressure was imposed at the outlet. The optimization problem was to minimize the total pressure drop between the inlet of the collector and the outlet of the combustion chamber with a constraint on the maximum temperature at the firing plate. The design variables were the area of the holes, the diameter of the central region, and the height of the holes. A variation in the proportion of the holes is acceptable. If the height is reduced, the holes must be scaled uniformly to maintain the shape.

The numerical domain consists of approximately 2.5 million polyhedral cells. The fluid domain only involves the methane circuit (assuming a supercritical fluid). The solid domain models the firing plate that is assumed to have a constant heat flow exchange with the combustion chamber.

Implementing the geometric parametrization

Mesh morphing techniques were used to geometrically parameterize both the holes and the height of the central region, while configurations involving enlargements of the central region were implemented by generating portions of fluid mesh subdomains to be activated appropriately. Two unstructured polyhedral mesh portions were generated and placed in the corresponding nominal domain positions. To allocate the new subdomains and create the required interface boundaries, the mesh was generated with slight refinement in the regions of the morphing actions. The largest domain was close to three million cells in size. The baseline geometry was obtained by deactivating the fluid subdomains, and setting to “wall” their boundary conditions. In the other configurations the boundaries of the active part were set as “interior” (the meshes on the interfaces of the hole domains were generated to be conformal to the boundaries of the main mesh).

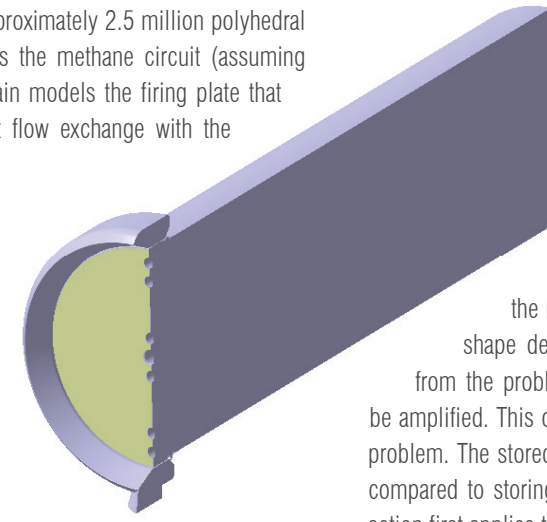


Fig. 2. Configuration of the fluid domain.

The RBF mesh morphing configurations

The RBF Morph mesh morphing tool was used to parametrize the area of the holes and the central height. The software uses radial basis functions as the mathematical framework to perform the smoothing action. This approach is widely recognized in the scientific community as one of the most efficient for performing this task. RBF Morph offers several tools to setup complex constrained parametrizations. It allows points to be extracted and controlled from the surfaces and edges of the domain, to be placed on primitive shapes (boxes, spheres, and cylinders), or specified directly with individual coordinates and displacements. Primitive shapes can be combined in a Boolean manner to limit the action of the morpher.

Shape information from a single RBF configuration is generated interactively using a GUI (graphical user interface) and subsequently used in batch commands that allow many shape modifications to be combined in a non-linear manner (non-linearities occur when rotation axes are present in the RBF configuration). The displacement of the prescribed set of source points, and the combination of RBF solutions, can be amplified according to parameters that constitute the parametric space of the model shape.

RBF Morph’s action is defined and executed by the following steps:

- setup – problems are defined and set up manually with the program GUI;
- fitting – the RBF system is solved for each morphing action and the solution stored to be available for amplification;

- smoothing – the surfaces and volumes of the computational domain are morphed according to the stored RBF solutions and arbitrary amplification factors.

The setup consists of defining the domain boundaries that restrict the morphing action; selecting the source points to be used to impose fixed and movable mesh regions; and prescribing the required movements of the points that will drive the shape deformation. In the fitting process the RBF, derived from the problem setup, is solved, and stored in a file ready to be amplified. This operation only needs to be performed once per RBF problem. The stored RBF solutions are very light (in terms of file size) compared to storing all the morphed meshes created. The smoothing action first applies the prescribed displacement to the grid surfaces and then uniformly propagates the deformation to the surrounding domain volume. It can be performed by combining several RBF solutions, each with its own amplification factor, to parametrically configure the computational domain.

Hole parameterization

Two RBF setups were implemented to change the area of the holes, one for each row of holes. The two setups are similar and only the position of the region of action differs (the position of the holes in the rows is not aligned). Both solutions are amplified with a single smoothing action. Each setup was performed on a single hole limiting the morphing to a volume surrounding its region. The setup was replicated on all other holes by exploiting a periodicity feature in the software. The hole scaling factor was set to use a unitary amplification value corresponding to an area twice the nominal geometry.

Height parameterization of the central region

Setting the RBF to change the height of the centre region involved a rigid translation of the walls of the centre region by selecting all nodes of its boundaries as source points. In this action the firing plate and injectors walls were kept unchanged. In conjunction with this rigid translation of the centre region, a so-called “two-step” morphing action was performed on the inlet holes. The two-step procedure consists of prescribing a displacement using a previously stored RBF solution as input. This technique allows better control of the displacement and provides a higher quality smoothing action. In our case the stored solution used as input consists of scaling the collector-side hole edge in a direction orthogonal to the hole axis and lying in the plane of the axis of symmetry. Since this direction is inclined with respect to the motor axis, the amplification factor is defined to maintain the same shape at both the inlet and outlet of the duct. The hole outlets are, in fact, scaled vertically by the displacement of the centre region. The RBF solution implemented locally on a single hole was applied to all the other holes using the periodicity feature. Fig. 3 shows the result of scaling the holes in the vertical direction.

Since the requirements for the shape of the inlet holes are different when increasing or decreasing the centre height, an additional RBF solution was set up to be amplified after hole displacement when negative

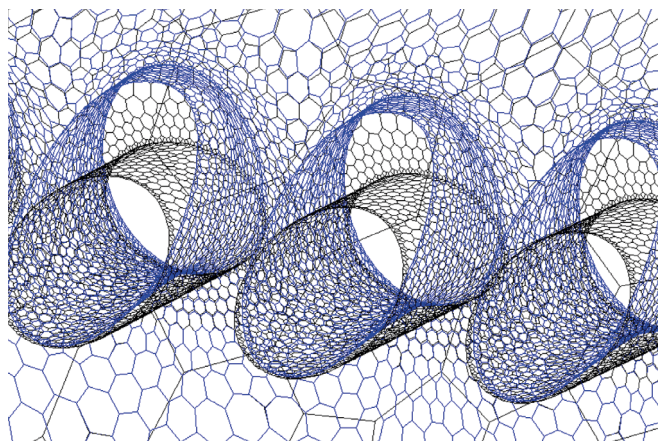


Fig. 3. Scaling of the inlet holes.

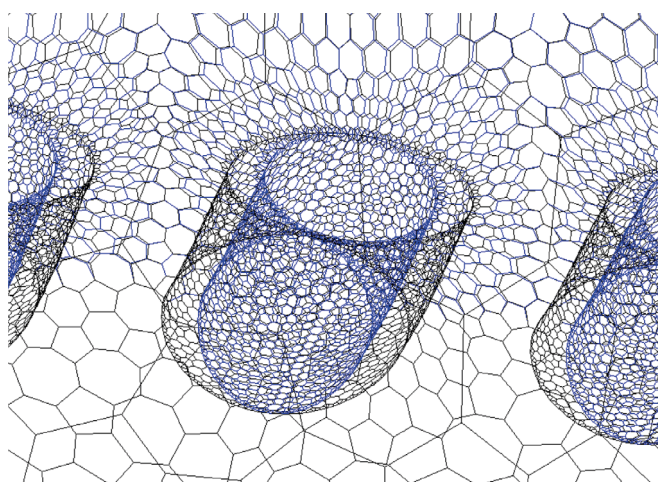


Fig. 4. Lateral scaling of inlet holes.

amplification occurs. It consists of scaling the holes in the tangential direction by a factor tuned to the translating amplification factor in order to recover the proportions of its shape. Fig. 4 details the scaling of the holes in the case of height reduction. A height reduction of more than 60% generates a very narrow region where the cells stretch to the point of degeneration. This limit was therefore assumed for the morphing action. The limit in the other direction is imposed by the presence of the manifold.

Optimization environment

The response surfaces constructed from the solutions of a DoE (design of experiments) table populated with 60 candidates were then optimized. A batch script evaluated the candidates by sequentially executing the calculations and storing the solutions in dedicated directories. For each run, a script loads the case, executes the mesh morphing sequences based on the input amplification factors, and performs 500 iterations. To accelerate the process all runs were restarted from a converged solution obtained on geometries with a nominal hole area and central height. A Linux cluster with 88 cores was used to perform the runs. The complete DoE table was calculated in approximately two days.

DoE table solutions

The performance indicators extracted from the computations were: the total pressure drop between the inlet and outlet of the domain, the

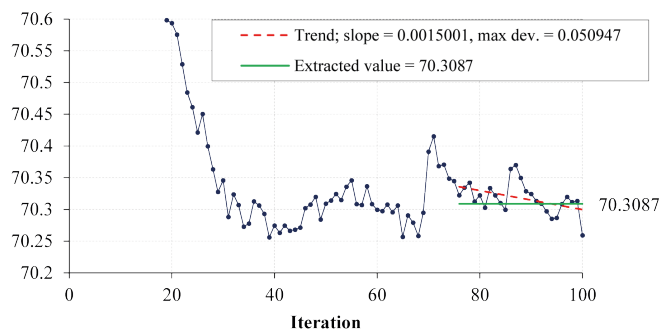


Fig. 5. Example of convergence history filtering.

maximum temperature of the firing plate, and the mass flow rate of all injectors. The convergence of the injector mass flow rates often showed irregular histories. In such cases, simply extracting the final number obtained by the calculation could prove misleading. A routine to filter the solutions was therefore developed and applied in extracting all the results.

It calculates a linearized interpolation of a final portion of the convergence history and takes a point in the final 25% of the segment as the solution of the calculation. The slope of the segment and the solution's maximum deviation therefrom are also evaluated. These values quantify the quality of the convergence obtained. Fig. 5 shows an example of how this filter works. In extracting the solutions of the design points to populate the DoE table, the last 50% of the convergence histories was evaluated.

Response Surface generation

The nature of the central region parameter, as a design variable, is somewhat differently considered to the other shape parameters. This parameter involves a change in geometric topology, so it is assumed to be a discrete variable that obtains the required values. In this scenario the optimization problem can be broken down into three separate optimizations based on two variables, an objective function, and a constraint. The matrix of the two continuous variables is regularly spaced and allows the generation of response surfaces based on a bicubic spline interpolations of orders 4 and 3 in the direction of the shift variable and hole area, respectively.

The procedure to select the optimum began by calculating the response surfaces for the maximum firing plate temperature. The isocurve at constant temperature was then extracted from the metamodel obtained. Fig. 6 shows the functions obtained for the cases corresponding to the three central hole diameters. The black dots correspond to the design points in the DoE table. The red curves are the selected isocurves.

The next step was to calculate the Response Surfaces for the total pressure drop. The previously selected isocurve variables were used to extract the corresponding curves on the new Response Surfaces. These curves constitute the functions on which to perform the minimization problem. The minimum of the minima of the three curves, corresponding to the three possible values of the central hole, is the optimal solution. Fig. 7 shows the pressure drop Response Surfaces and the constrained curve (in blue) used to select the minima.

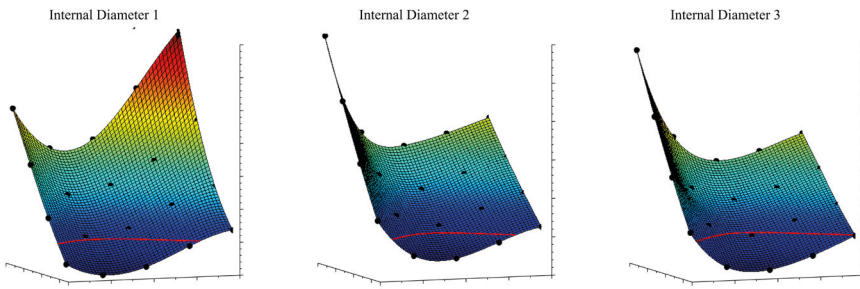


Fig. 6. Response Surfaces for the maximum firing plate temperature.

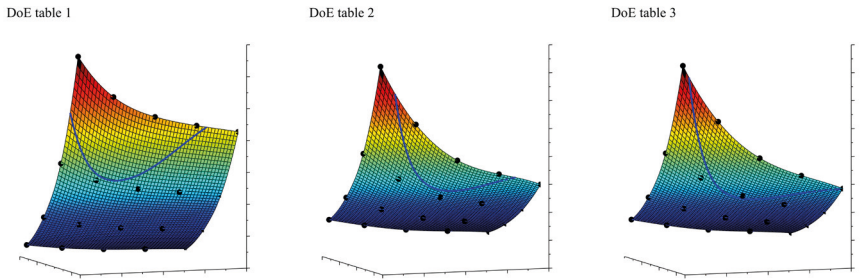


Fig. 7. Response Surfaces for total pressure drop.

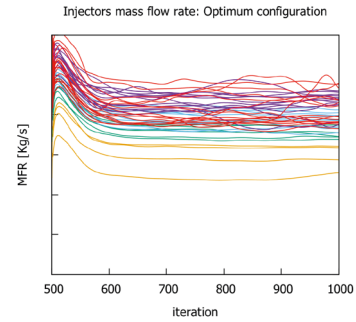
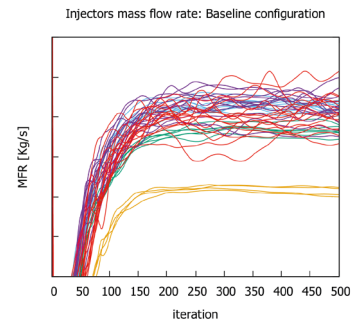


Fig. 8. Convergence histories of the injector mass flow rates.

Verification of the optimum

The identified optimum has a 29.5% reduction in pressure drop, compared to the baseline configuration (calculated from the developed metamodel). In order to confirm this performance, the optimum candidate was analysed using the workflow for calculating the design points in the DoE table, and imposing the variables extracted from the Response Surface as amplification factors. The solutions obtained were compared to the solution of the baseline configuration. The improvement estimated is confirmed to be very close to 30%. Compliance with the constraint of maximum firing plate temperature is also confirmed.

Injector mass flow rate (MFR) statistics

The mass flow rate through the injectors was monitored by surfaces at the interfaces between each injector outlet and the combustion chamber inlets. As already mentioned, the convergence histories of the mass flow rate often showed significant irregularities. Fig. 8 shows the MFR convergence histories of all injectors for both baseline and optimum configuration calculations. The observed irregularities justify the application of the extraction filter solution developed.

Fig. 9 shows the slope values of the linearized interpolation of the convergence histories of all injector mass flow rates as well as the maximum deviation from the trend. The statistics concern the calculation performed on the baseline configuration. The same analysis on the optimized configuration is shown in Fig. 10. To facilitate comparison, the solutions are plotted with the same scale. The statistics suggest a slightly smoother convergence behaviour for most of the optimized configurations' injectors.

Both solutions, however, show mass flow fluctuations – especially on the outermost injectors. The mass flow rate values extracted by applying the filter are shown for both the baseline and optimized configurations in Fig. 11. The standard deviation of the MFR of the injectors from the

average of the optimal configuration is about 24% lower than the baseline value. Much of the contribution to this more uniform mass flow rate distribution can be attributed to the higher flow in the internal injectors enabled by the optimized geometry.

What we achieved

The constrained numerical optimization procedure described allowed us to identify a geometric configuration for the engine injector head capable of reducing the pressure drop between the inlet and the outlet of the methane circuit by approximately 30% compared to the baseline geometry. The optimal solution was also shown to allow a slightly more even distribution of the methane mass flow rate through the various injectors, although some flow irregularities are still present mainly in the outer injectors. Figs. 9 and 10 compare the statistics of the baseline

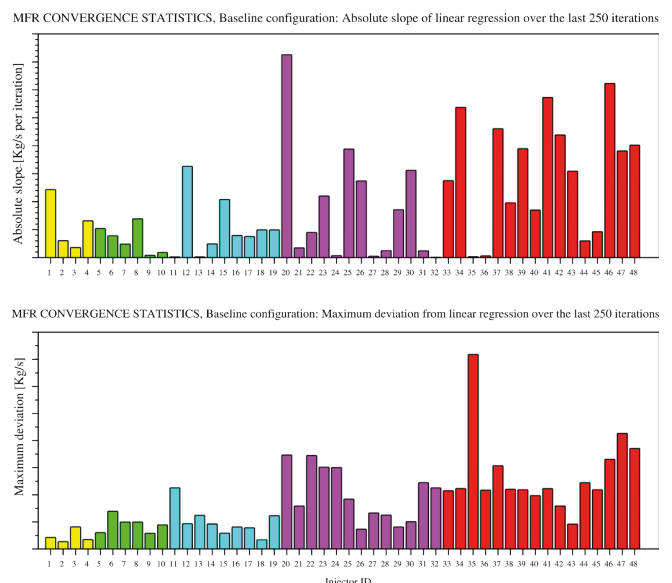


Fig. 9. Statistics of MFR convergence histories of the baseline configuration.

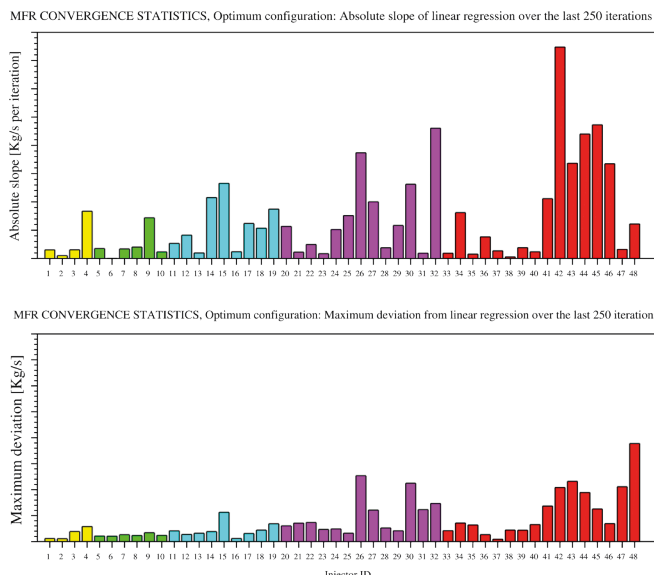


Fig. 10. Statistics of MFR convergence histories of the optimal configuration.

and the optimized geometries. Fig. 11 compares the mass flow rate through the different injectors. The mesh morphing technique used to parameterize the geometry proved to provide a very robust and efficient numerical model. None of the morphing actions performed on the 60 candidates in the DoE tables failed to provide a valid geometry, and none of the fluid dynamics calculations failed to generate a convergent solution.

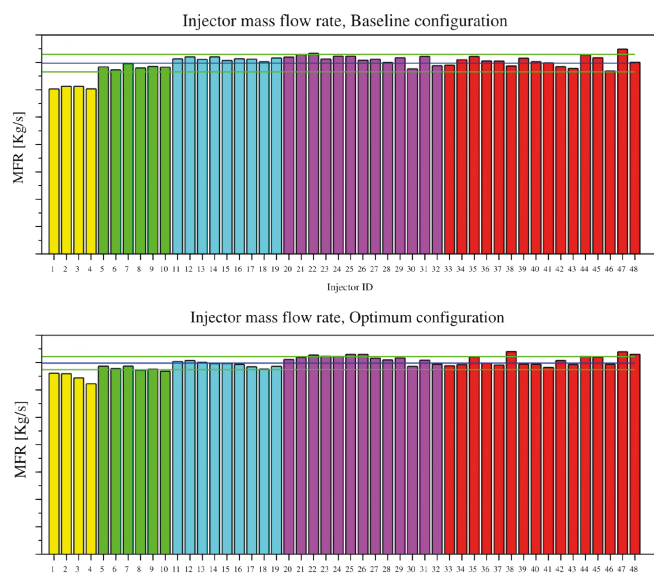


Fig. 11. Injector mass flow rates of the baseline and optimized configurations.

About RBF Morph

RBF Morph is a unique mesh-morphing technology that combines very accurate control of the geometrical parameters with extremely fast mesh deformation, fully integrated into the solving process. Our mission is the development and broad application of simulation technology to synthesize and optimize designs, processes and decisions for our clients that need better performance in less time. www.rbf-morph.com

The DoE approach and generating a metamodel of the objective function simplified the selection of the constrained optimum whose performance was confirmed by a post design verification analysis.

The outcomes of the optimization activity described contributed to the configuration of a new engine that was successfully tested at Avio's new Space Propulsion Test Facility (SPTF) at Salto di Quirra in Sardinia in Italy.

Tools used

The software used in this activity was:

- RBF Morph
- Ansys Fluent
- Ansys Meshing
- Ansys optiSLang

Acknowledgment

A special acknowledgement to ESA for providing VEGA E material, data, and figures.

For more information:

Ubaldo Cella – RBF Morph
ubaldo.cella@rbf-morph.com

About Avio

Avio is a leading company in space propulsion based in Colleferro (Rome). The expertise and know-how acquired in over 100 years in explosives and more than 50 in space activities allow Avio to compete with the top players in the Space Launch Systems definition and integration as well as in the segment of solid, liquid and cryogenic space propulsion. Today, Avio plays a strategic role in the global space industry through VEGA. The Combustor Engineer department, part of the Liquid Propulsion Department, is focused on combustor design and Additive Layer Manufacturing (ALM) technologies.

About ESA

European Space Agency's (ESA) mission is to shape the development of Europe's space capability and ensure that investment in space continues to deliver benefits to the citizens of Europe and the world. ESA is an intergovernmental organization of 22 member states. By coordinating the financial and intellectual resources of its members, it can undertake programmes and activities far beyond the scope of any single European country. ESA's programmes are designed to find out more about Earth, its immediate space environment, our Solar System and the Universe, as well as to develop satellite-based technologies and services, and to promote European industries. ESA also works closely with space organisations outside Europe.